

Computer Aided Morphological Analysis for maxillo-facial diagnostic: a preliminary study

Original

Computer Aided Morphological Analysis for maxillo-facial diagnostic: a preliminary study / Calignano, Flaviana; Moos, Sandro; Vezzetti, Enrico. - In: JOURNAL OF PLASTIC, RECONSTRUCTIVE & AESTHETIC SURGERY. - ISSN 1748-6815. - (2008), pp. 218-226. [10.1016/j.bjps.2008.09.031]

Availability:

This version is available at: 11583/1843765 since:

Publisher:

ELSEVIER

Published

DOI:10.1016/j.bjps.2008.09.031

Terms of use:

openAccess

This article is made available under terms and conditions as specified in the corresponding bibliographic description in the repository

Publisher copyright

(Article begins on next page)

Computer aided morphological analysis for maxillo-facial diagnostic

Abstract

This paper compares most of the 3D morphometric methods currently proposed by the technical literature to evaluate their morphological informative value, applying them to a case study of five patients affected by the Malocclusion pathology. The methods compared are: Conventional Cephalometric Analysis (CCA), Generalized Procrustes Superimposition (GPS) with Principal Component Analysis (PCA), Thin-Plate Spline analysis (TPS), Multisectional Spline (MS) and Clearance Vector Mapping (CVM).

The result shows that Multisectional Spline (MS) satisfy better the need of reliable and useful diagnostic information.

Key words: 3D Scanner, Shape analysis, Facial Morphology

1 Introduction

2 The assessment of the dimensions and arrangement of facial soft tissues is
3 important for medical evaluations. Orthodontists, orthognathic maxillofacial
4 and plastic surgeons often require quantitative data about the correlation
5 between soft and hard tissues [1,2].

6 For many years these information have been obtained from 2D radiographies
7 and photos, even if these have been consistently limited [1,3,4,5,6]. Significant

8 improvements have been obtained with the use of computer vision algorithms,
9 even if the use of bidimensional supports to analyze three-dimensional objects
10 seems to be quite inadequate.

11 For this reason, many research efforts of the last ten years have been directed
12 to develop computer vision tools, that with the use of 3D scanner devices are
13 able to provide reliable and more complete data. These systems use different
14 technologies, like active or passive light reflection analysis and are able to
15 describe 3D real shapes with a point cloud, analyzable with 3D software.

16 But while the image processing methodologies are well known in the medical
17 context, the situation for the 3D scanner is still quite marginal and fragmented.
18 Some studies have been developed for proposing a structured procedure that
19 could be used for driving the physician in the application of 3D scanner to
20 medical diagnosis [7,8,9,10,11,12]. No one succeeded in the development of a
21 standardized strategy and accepted by the whole medical context but, con-
22 trarily, the more employed methodology for the maxillo-facial diagnosis is still
23 the conventional cephalometric analysis (CCA), that employs bidimensional
24 radiographies.

25 Considering the necessity to support the development of a standardized pro-
26 cedure able to employ 3D data for an useful and reliable diagnosis for maxillo-
27 facial pathologies, this paper proposes a first analysis of the advantages and
28 limitations of the methods proposed in the technical literature. Without giving
29 a clear and structured comparison of the different approaches, it's impossible
30 to successfully develop a standardized methodology.

31 **2 Methods synthesis**

32 A short description of the methods applied to the study case is presented. The
33 Conventional Cephalometric Analysis is widely employed although it still re-
34 lies on 2D radiographies. The Generalised Procrustes Superimposition (GPS)
35 and the Thin-plate spline analysis (TPS) are the two most important mor-
36 phometric analysis techniques. Then are described the Multisectional Spline
37 (MS) and the Clearance Vector Mapping (CVM) methods that treat the 3D
38 information of the point clouds.

39 *2.1 Conventional cephalometric analyses (CCA)*

40 The use of conventional measurements in traditional cephalometric analyses
41 is called Conventional Cephalometric Analysis (CCA) [11]. A set of linear
42 distances and angles is measured between reference points (landmarks), laid
43 on lateral radiographies. The CCA measures are processed with statistical
44 methods like PCA, ANOVA, paired T-tests and F-tests to compare groups of
45 patients [13].

46 *2.2 Geometrical morphometrics*

47 The use of geometrical morphometric tools in the shape analysis is also known
48 as “statistical shape analysis”. The two following techniques are the most
49 important.

50 2.2.1 Generalised Procrustes superimposition (GPS) and Principal Compo-
51 nent Analysis (PCA)

52 The Generalised Procrustes analysis can be used to compute, visualize and test
53 the morphological differences between facial profiles. It's an iterative method
54 that apply geometrical transformations like scales, translations, rotations and
55 reflections, in order to compare reference points (landmarks) [14] that can
56 be taken from different point clouds of the patient's face. For visualization
57 purposes, sometimes the landmarks appear linked by straight lines, that have
58 no effect on computations.

59 As first step, the average facial profile (consensus) it's calculated and it's
60 possible to evaluate anthropometrical measures on it (fig. 1). As second step,
61 it's usually performed a Principal Components Analysis in order to point out
62 the morphological differences of the various facial profiles from the consensus.

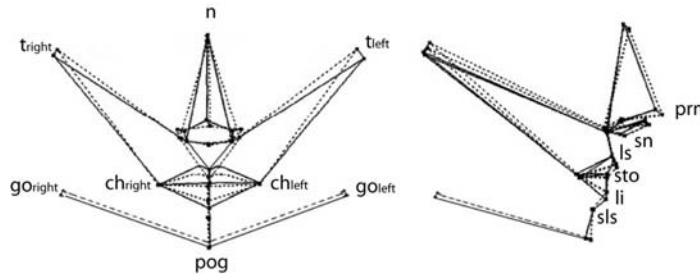


Figure 1. Examples of GPA “Consensus” evaluation.

63 The Principal Component Analysis (PCA) evaluates the tendency of the land-
64 marks distribution along x and y axis, locating a new working frame, centred
65 on the average shape centre. The method creates new variables named prin-
66 cipal components (PCs), that describe how much the landmark configuration
67 of each sample is different from the average shape.

68 2.2.2 *Thin-Plate Spline analysis (TPS)*

69 This method works on 2D radiographies taken before and after the surgery
70 treatment on the patient. Firstly, a point set of anatomical landmarks is de-
71 fined on both of them; then the post-surgery radiography is considered as
72 an infinitely thin metal plate that must be bended, in a direction orthogonal
73 to the plane, in order to match its landmarks to the pre-surgery radiography,
74 while the bending energy it's minimized [15,16]. If the two shapes are identical,
75 the bending energy is zero and the plate is flat.

76 The choice of the spline function depends on mathematical properties rather
77 than relevant biological data [11], but the result is a rigorous quantitative
78 analysis of the spatial shape changes [17].

79 2.3 *Multisectional Spline (MS)*

80 To give information regarding the face morphology also in the regions around
81 the landmarks, this approach employs section planes passing through a set
82 of specific reference points of a point cloud (landmarks), in order to obtain
83 a specific section spline. The shifts of the facial morphology between the pre
84 and post surgery point clouds can be analyzed by comparing the two section
85 profiles passing through homologous landmarks and section planes [18,19].

86 2.4 *Clearance Vector Mapping (CVM)*

87 While both the previous methods manage little portion of the point cloud sep-
88 arately, the Clearance Vector Mapping (CVM) is able to analyze the global

89 morphological information of the point cloud [20], so to provide a more com-
90 plete information of the face morphology behavior.

91 The pre and post surgery point clouds are firstly aligned using different kind
92 of alignment algorithm such as ICP, CSM, ... [21] or using a combination of
93 the three invariant points of the Frankfort plane: tr (tragion of the ears) and
94 or (orbital of the eyes).

95 Then, the magnitude of the 3D shape displacement can be computed work-
96 ing on triangulated meshes and following different approaches [22]: *radial*, if
97 the distance between the two surfaces is measured along a ray starting from
98 the centroid of the pre-surgery surface; *normal*, if the distance between the
99 acquired surfaces is measured along the direction of the local normal of the
100 pre-surgery scan and *closest*, if the distance between the two surfaces is mea-
101 sured searching the closest point on the post-surgery surface, starting from a
102 pre-surgery point.

103 The magnitude of the displacement between the pre and post surgery point
104 clouds is shown with a colour mapping.

105 **3 Case Study selection**

106 *3.1 Identification of the facial pathologies*

107 The selection of the facial pathology has been driven by the necessity of a
108 simple surgery treatment to allow a simple understanding of the correlation
109 between hard tissue modifications and soft tissue shifts. If the case study would
110 analyze a pathology treated with many surgical hard tissues modifications, it

111 would be very difficult to obtain a clear idea of the correlation between the
112 resulting soft tissue shift due to an hard tissue displacement.

113 The selected facial pathology is the “malocclusion”, characterized by a mis-
114 alignment between upper and lower mandibular structures (fig. 2), that causes
115 significant mastication problems. It is treated with a surgical translation of
116 the mandible.

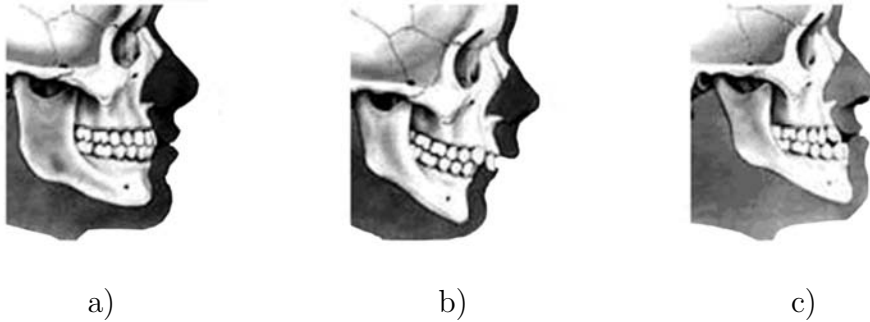


Figure 2. Schematic example of malocclusion: a) Class I, b) Class II, c) Class III.

117 In this paper are analyzed patients affected by class I and class II malocclusion.

118 *3.2 3D scanner device*

119 For the methods requiring 3D point clouds, the acquisitions were made working
120 with a 3D laser scanner Cyberware Scanner 3030RGB (fig. 3). The five patients
121 have been digitized before and after the surgery treatment.

122 *3.3 Morphological measures*

123 All the morphological analysis methods have been compared to the consoli-
124 dated conventional chephalometric method.

125 Two measures families of significant anthropometric points (landmarks) have

126 been evaluated over the facial shape to perform a reliable and consistent com-
 127 parison of the methods.

128 The first family of measures have been evaluated over the soft-tissue shape
 129 points for those who employ the 3D scanner devices and work on external
 130 surfaces, while the second one refers to points on hard (skeletal) tissues for
 131 those methods who employ radiographies.

132 Although some methods employ the first measures family, while others use the
 133 second one, the comparison will be at the same possible and reliable because
 134 soft tissue reference points overlap the hard tissue reference points, with a
 135 known shift given by the average thickness of the facial soft tissue.

136 For each patient the three-dimensional coordinates of the 16 facial soft tissue
 137 landmarks (fig. 4a) and of 8 hard tissue landmarks, on the cranium, (fig. 5a)

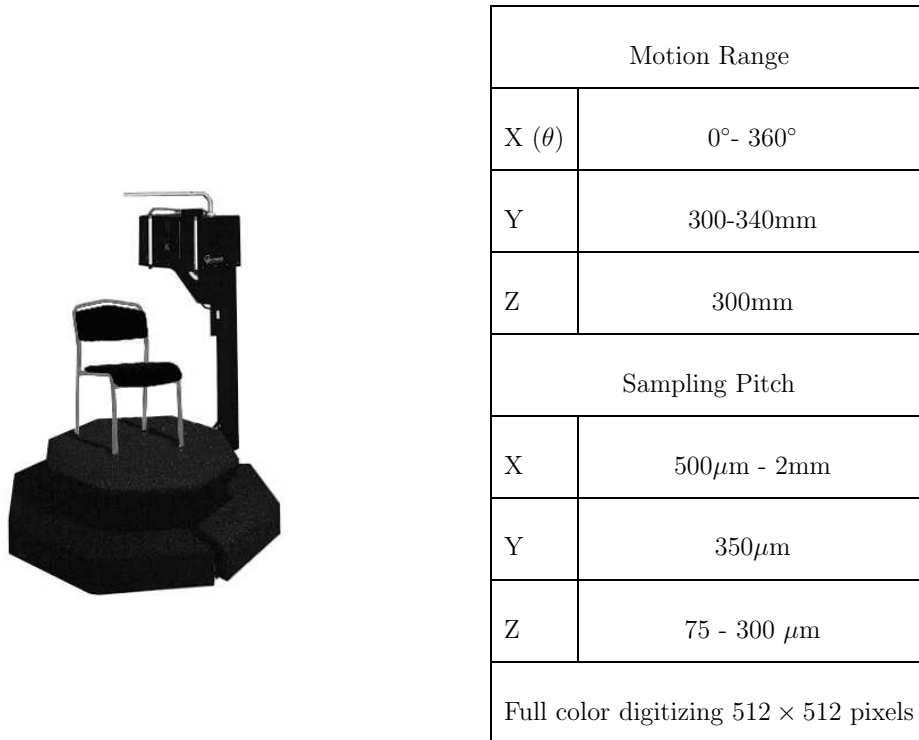


Figure 3. Cyberware 3D laser scanner 3030RGB (Cyberware Lab. Inc., Monterey, California)

138 have been identified on point clouds and lateral cephalometric radiographs
 139 respectively. They are listed in table 1.

Table 1

List of soft and hard tissues morphological reference points (landmarks).

Soft tissue landmarks		Hard tissue landmarks	
Name	Abbr.	Name	Abbr.
Nasion	n	Nasion	N
Pronasale	prn	Menton	Me
Subnasale	sn	Anterior Nasal Spine	SNA
Labiale superius	ls	Gnathion	Gn
Stomion	sto	Articulare	Ar
Labiale inferius	li	Gonion	Go
Sublabiale	sls		
Pogonion	pog		
Tragion	t_{right}, t_{left}		
Nasal alar crest	al_{right}, al_{left}		
Cheilion	ch_{right}, ch_{left}		
Gonion	go_{right}, go_{left}		

140 The (x, y, z) coordinates of the landmarks have been used to calculate a set of
 141 three-dimensional soft tissue measurements (figg. 4b and 4c), following [23,24]
 142 where they was applied to a reference group of 153 men with no previous
 143 history of craniofacial injury or operation, or congenital abnormalities. Pre-
 144 cisely, the measures here considered are the mandibular corpus length ($pg -$
 145 go_m), the anterior lower facial height ($sn - pg$), the lower facial width (go_{right}

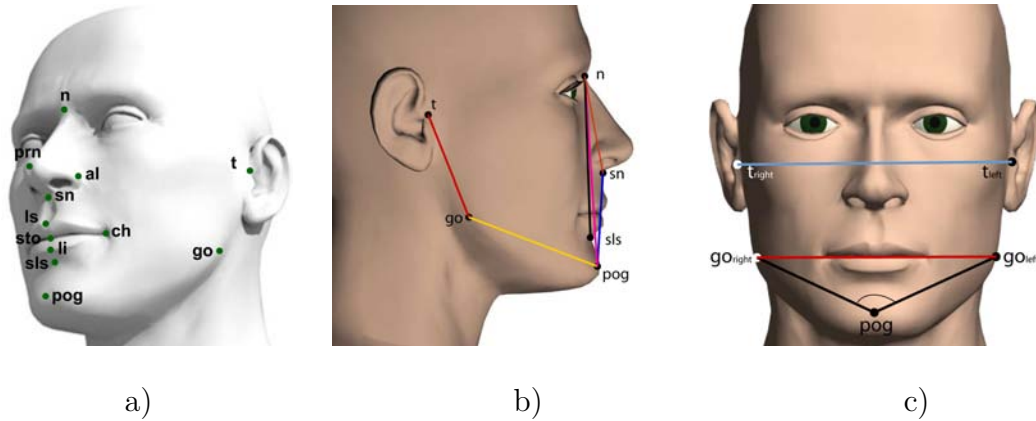


Figure 4. a) Graphical location of soft tissue landmarks. b) and c) Three-dimensional soft tissue measurements.

146 – go_{left}) and the nose width ($al_{right} - al_{left}$). Each “landmark_m” is derived as
 147 the mid-point between two homologous landmarks.

148 Some important measurement ratios are also considered, like the facial width
 149 to facial height ratio $(t_{right} - t_{left}) / (n - pog)$ and the posterior facial height to
 150 anterior facial height ratio $(t_m - go_m) / (sn - pog)$. Some angular measures are
 151 considered to complete the description: the mandibular convexity ($\widehat{go_{right} pog}$
 152 go_{left}), the maxillary prominence relative to the mandible ($sls \hat{n} sn$) and left
 153 and right goniac angles $(t_{left} \widehat{go_{left} pog})$, $(t_{right} \widehat{go_{right} pog})$.

154 Similarly, the cephalometric angular and linear measurements can be defined
 155 also for anatomical hard tissue landmarks (figg. 5b, 5c). The linear measures
 156 here considered are the facial height of the anterior face ($N - Me$), the anterior
 157 upper height of the face ($N - SNA$), the anterior lower height of the face (SNA
 158 $- Me$), the posterior height of the face ($S - Go$), the upper posterior height
 159 of the face ($S - Ar$), the lower posterior height of the face ($Ar - Go$). The
 160 angular measurements are defined by the intersection of lines passing through
 161 landmarks, such as $(ArGo - GoGn)$ who describe the slope of the mandibular
 162 plane relative to the anterior base of the skull as angle between the $(Ar - Go)$

163 line with the mandibular plane (Go – Gn) and the Gnathion angle (ArGo –
164 GoMe) who describes the slope of the ramous relative to the mandible body
165 as angle between the (Ar – Go) line with (Go – Me) line

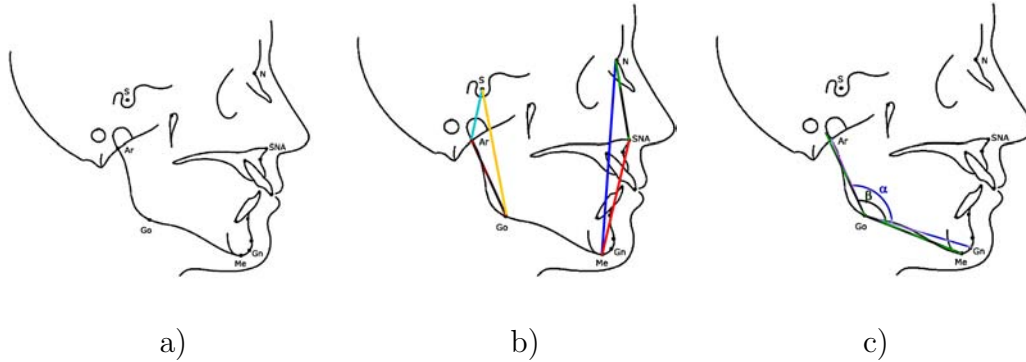


Figure 5. a) Graphical location of hard tissue landmarks. b) Landmark linear distance and c) landmark angular distances.

166 4 Experimental comparison of the morphological methods

167 The 3D scanner was set-up with the most efficient parameters for the face
168 acquisition and the five different patients were digitized before and after the
169 surgery treatment. The evaluations methods, proposed by the technical liter-
170 ature, have been applied to the ten points clouds and their result have been
171 compared to the conventional cephalometric approach (CCA), usually em-
172 ployed for facial malformation pathologies diagnostic.

173 The data here presented were measured on later cranial radiographies (fig. 6),
174 that are normally employed by the physician to evaluate the soft tissue move-
175 ments and will be used as first comparison term for the other morphological
176 methods, in order to give the physician a more clear idea of their advantages
177 and disadvantages.

178 It is possible to see in table 2, that after the surgery treatment the lower part
 179 of the facial profile (SNA – ME) has increased its length, with a consequent
 180 reduction of the upper part of the face (N – SNA). This is also confirmed
 181 by the Index of Anterior Facial Ratio (iPFA), namely the ratio between (N
 182 – SNA) and (SNA – ME), that decreases its value from the value of 0.85 in
 183 the pre surgery face profile, to the value of 0.75 in the post surgery. Following
 184 the medical standards proportions (N – SNA) represents the 45% of the total
 185 facial length and (SNA – ME) is the 55%.

186 In the case studies analyzed in the pre surgery morphology the proportions
 187 are maintained, but not in the post surgery, where the evaluated differences
 188 from the standard percentage are around 3%.

189 In order to verify the mandibular modification with other measures, the goniac
 190 angle β has been measured. Moving from pre to post surgery facial shape, this
 191 value has shown a significative increasing probably due to the rise of the mea-
 192 sure (Ar – Go). To verify this hypothesis, the goniac angle β has been divided
 193 in two parts: the lower and upper goniac angle, that have been separately

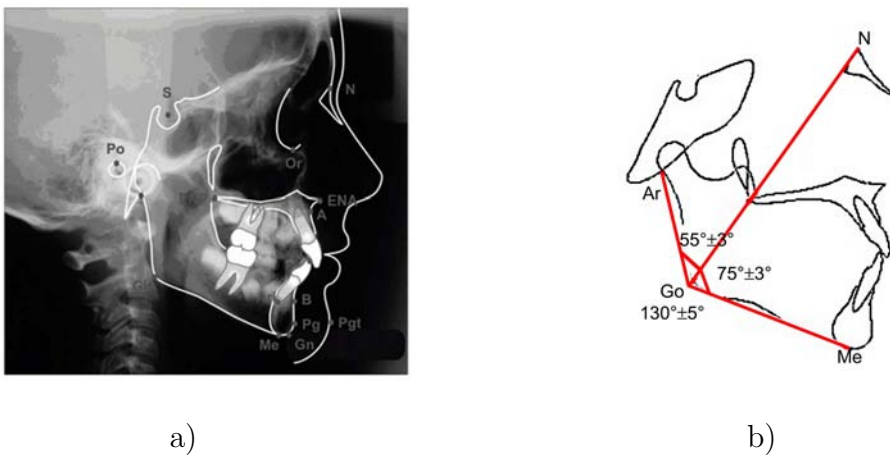


Figure 6. a) One instance of later cranial radiography. b) Lower and upper goniac angles with standardized values.

194 evaluated. Figure 6b shows the two angles and their standard values.

195 The calculated values are in table 3. The ratio between standard deviation σ
 196 and average value μ , of the two portions of the goniac angles also show that
 197 the lower goniac angle has a more stable behaviour, so it could give more
 198 reliable information about the facial shift between pre and post surgery.

199 Both in the pre and post surgery the measured angles are different from the
 200 standardized values (fig. 6b): the upper goniac angle is bigger than 55° , while
 201 the lower goniac angle is lower than 70° , but the surgery treatment has caused
 202 an horizontal increasing of the mandible measures, bringing it towards more
 203 normal values.

Table 2

Angular and linear cephalometric measures with the significance analysis of pre and post surgery facial morphology modifications (Average μ , Standard deviation σ).

Dimensions in mm.

Measure	Pre-surgery					Post-surgery					Significance analysis		
	Face 1	Face 2	Face 3	Face 4	Face 5	Face 1	Face 2	Face 3	Face 4	Face 5	μ	σ	σ/μ
ArGo-GoGn (α)	130.02	134.76	148.52	136.51	131.30	134.67	134.36	152.19	136.19	129.80	1.22	2.74	2.251
ArGo-GoMe (β)	136.26	139.10	151.37	138.65	132.49	139.81	140.00	156.60	139.16	136.08	2.75	1.99	0.72
S-Go	68.88	75.77	71.95	62.66	62.01	90.17	71.29	57.48	61.02	64.25	0.58	13.12	22.32
N-Me	126.68	111.95	135.35	117.36	116.36	125.22	110.80	126.41	116.58	124.53	0.83	6.07	7.29
N-SNA	68.53	64.84	64.21	57.85	54.47	52.72	58.86	59.54	58.29	58.28	4.44	7.48	1.68
SNA-Me	70.44	64.29	88.04	72.33	67.93	82.46	64.96	87.08	72.76	77.43	4.33	5.97	1.38
S-Ar	16.60	16.55	22.95	17.25	17.31	18.48	13.58	16.12	15.82	14.60	2.41	3.14	1.3
Ar-Go	65.37	57.95	55.14	59.40	48.57	67.93	58.03	44.68	59.50	51.99	0.86	5.57	6.47

Table 3

Measures of Lower and Upper goniac angles (Average μ , Standard deviation σ).Dimensions in degree.

Measure	Pre-surgery					Post-surgery					Significance analysis		
	Face 1	Face 2	Face 3	Face 4	Face 5	Face 1	Face 2	Face 3	Face 4	Face 5	μ	σ	σ/μ
Ar \widehat{Go} N	72.57	77.37	77.09	73.72	64.29	72.34	71.81	80.69	71.91	69.38	0.22	4.27	19.58
N \widehat{Go} Me	66.98	62.69	74.50	64.10	72.48	63.95	65.66	74.15	62.80	68.85	1.07	2.61	2.45

204 4.1 Generalised Procrustes Analysis (GPA)

205 The graphical results of the Procrustes superimposition are shown in figure 7.

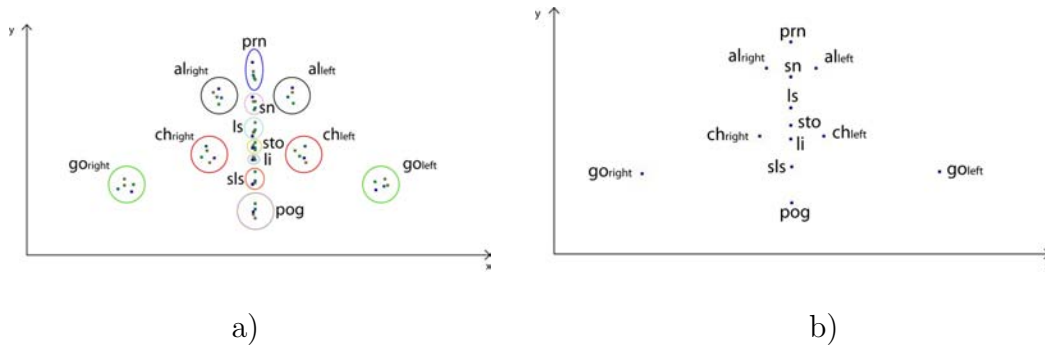


Figure 7. Graphical GPA analysis output: a) Procustes fitting, b) average shape (Consensus).

206 The method also provides the sum of squares, mean squares, the residual
 207 values and a Fisher test in order to show which transformation has been
 208 significant for the average shape evaluation. The values of table 4 show that
 209 the most significant contribution over the entire average shape evaluation is
 210 the translation, immediately followed by the rotation and scaling.

211 In the analyzed case studies, the PCA approach has given evidence that in the
 212 pre-surgery facial shape the 84,78% of the entire shape modification presents
 213 a more significant tendency along the x axis, 45.65% of the points cloud em-
 214 ployed for the average evaluation, than along y . This situation seems to be

215 maintained quite constant also in the post-surgery shape, with 43.93% along x
 216 and 37.58% along y . Comparing the average shapes, with the PCA graphical
 217 synthesis, of pre and post surgery (fig. 8) it is possible to see that there is a sig-
 218 nificant compression of the nose-labial region, as verified with the traditional
 219 cephalometric approach cited in the previous paragraph.

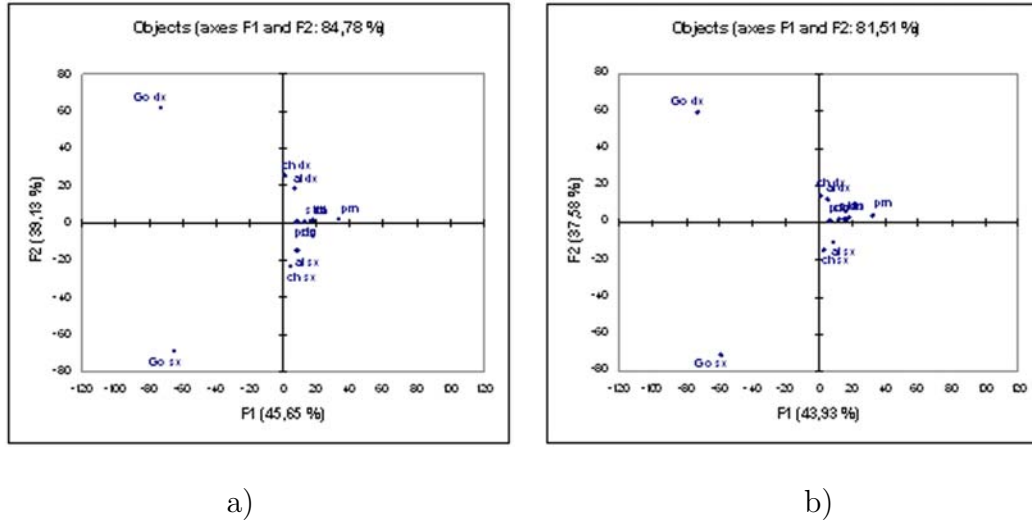


Figure 8. PCA outputs: a) PCs pre-surgery; b) PCs post-surgery.

Table 4

Procrustes Analysis case study evaluation (DF Residuals, S.S. Sum of Squares, M.S. Mean Squares). Dimensions in mm.

Source	Pre-surgery					Post-surgery				
	DF	S.S.	M.S.	F	$Pr > F$	DF	S.S.	M.S.	F	$Pr > F$
Residuals after scaling	128	2921.93	22.83			128	6855.6	53.56		
Scaling	4	47.78	11.95	0.52	0.719	4	431.05	107.76	2.01	0.097
Residuals after rotation	132	2969.71	22.5			132	7286.65	55.2		
Rotation	12	602.44	50.2	2.2	0.015	12	21150.01	1762.5	32.91	< 0.0001
Residuals after translation	144	3572.15	24.81			144	28436.66	197.48		
Translation	12	3515.85	292.99	12.84	< 0.0001	12	2657.24	221.44	4.13	< 0.0001
Corrected Total	156	7088.01	45.44			156	31093.9	199.32		

220 But while the traditional standardized approach underlines that the Gonion
221 (Go) location has been moved down from the pre-surgery location, the results
222 of this approach shows an opposite translation, giving a wrong information.
223 The graphical synthesis employed by this method, wich considers only the
224 landmark points, is not able to provide information about the global soft tis-
225 sue shape variation. Making more than one test, about the repeatability of
226 the method, it has been evidenced that the approach needs a precise selection
227 of the correct landmark location. If during the method implementation the
228 operator does not locate precisely the real landmark, but only a close point,
229 the method will evaluate the average figure including the erroneous point and
230 this will also affect the consesus. Instead, the traditional approach [25,26]
231 provides more reliable information because the selection of an erroneous land-
232 mark in the definition of a reference plane, for example the Po in defining the
233 Frankfort horizontal, will be clearly evident in the morphological and graph-
234 ical evaluation outputs (for example the Frankfort-mandibular plane angle,
235 the Frankfort-mandibular incisor angle, the facial angle . . .) [27].

236 Finally, in the Procrustes method are defined several approach [28], particu-
237 larly for the shape scaling, that leads to significant different results. This has
238 been verified using different commercial software.

239 4.2 *Thin Plate Spline (TPS)*

240 The Thin Plate Spline method is a chephalometric approach as the CCA. For
241 this reason the evaluation of its performances has been developed employing
242 the hard tissues landmarks. Thin-plate spline algorithm computes the orthog-
243 onal least-squares Procustes average configuration of landmarks in group at

244 pre and post treatment using the generalized orthogonal least-squares [29].
245 The average craniofacial configurations has been subjected to TPS analysis
246 by contrasting the average configuration at post-surgery with that at pre-
247 surgery. The total spline is then decomposed into affine and non affine compo-
248 nents. The affine transformation provides information about size differences,
249 rotation and uniform shape change. Non-affine transformations delineate non-
250 uniform or local deformations. These can be further decomposed into localized
251 components, represented by partial warps corresponding to deformations at
252 different geometrical scales. The partial warps have anatomical interpretabil-
253 ity and they are necessary to understand the statistical significance of the
254 overall shape changes (fig. 9).



Figure 9. Graphical display of pre and post comparison: craniofacial shape changes with TPS approach.

255 The graphical output of non affine transformation principal component has
256 shown, as the previous method, a slight compression in the vertical axis in
257 the anterior region of the maxilla, and an extension in the mandibular region.
258 The partial warp with the largest magnitude has confirmed the compression
259 in the anterior part of the maxilla and the extension in the chin area. While
260 the Procrustes method has given only partial reliable information about the

261 soft-tissues changes between pre and post surgery this strategy seems to be
262 more reliable showing the same shifts evidenced in the CCA.

263 This method gives limited visual information about the facial morphology
264 shifts because it could only separately analyze the lateral or frontal facial
265 profiles. Considering the necessity to give simple and direct information to the
266 physician this method seem to be quite limited in relation with the complexity
267 of the graphical output evaluation.

268 4.3 Multisectional Spline

269 The objective of the method is to define bidimensional section profiles on the
270 pre and post surgery point clouds and to perform on them cephalometric
271 measures. An example of output is shown in figure 10, while the results are
272 listed in table 5.

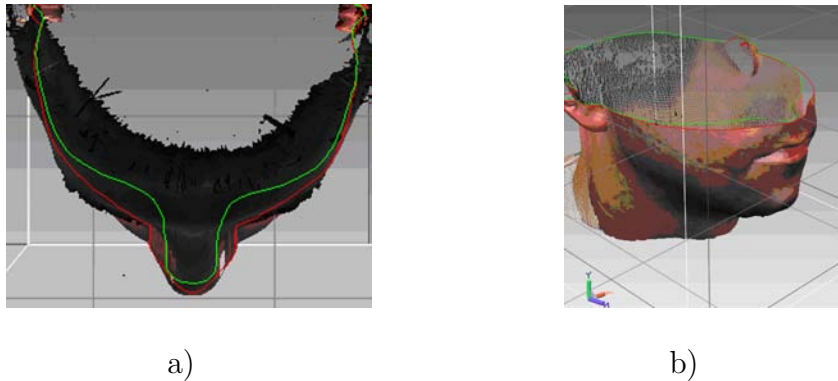


Figure 10. Multisectional spline output on: a) xz plane section b) yz plane section (green colour for pre surgery profile and red colour for post surgery profile).

273 The results of the sectioning show a significant asymmetry between the right
274 and left side of the patient, both before and after the surgery treatment. This
275 information is found the first time using this method because the section pro-
276 files are more suitable to describe the global facial shifts than the other meth-

ods [30]: CCA and TPS works only on planar radiographies and GPA/PCA works only on a point set so it is difficult to obtain global information.

Table 5

Pre and post-surgery cephalometric measures comparison for Multisectional Spline method and significance analysis (Average μ , Standard deviation σ). Dimensions in mm.

	Ref. value	Pre-surgery					Post-surgery					Significance analysis		
		Face 1	Face 2	Face 3	Face 4	Face 5	Face 1	Face 2	Face 3	Face 4	Face 5	μ	σ	σ/μ
$pog - g_{om}$	82	102.26	80.23	96	100	92.69	109.31	83.58	84.98	103	78	2.46	9.71	3.94
$sn - pog$	55	59.44	45.89	58.69	49.55	59.40	54.86	49.01	59.64	48.97	61.04	0.11	2.94	26.73
$g_{oright} - g_{oleft}$	116	140.26	123.14	133.18	126.52	127.98	144.86	128.77	128.57	122.59	131.76	1.09	4.95	4.52
$a_{right} - a_{left}$	36	37.83	31.86	40.44	39.01	40.35	33.12	29.36	37.37	34.86	30.91	4.77	2.75	0.57
$g_{oright} - \widehat{pog} - g_{oleft}$	71	84.80	82.23	98.64	77.98	91.05	85.38	82.85	93.83	80.65	92.32	0.07	2.85	43.24
$sls - \widehat{n} - sn$	12	7.83	8.67	7.51	9.10	11.84	8.57	8.06	3.69	7.60	21.29	0.85	5.09	5.97
$t_{right} - g_{oright} - pog$	130 ± 6	132.26	135.92	145.84	129.13	132.47	131.61	134.25	139.55	132.18	134.89	0.63	3.74	5.96
$t_{left} - g_{oleft} - pog$	130 ± 6	134.84	136.72	141.85	137.33	136.04	136.17	137.92	139.55	136.56	133.05	0.71	1.97	2.79
$(t_{right} - t_{left})/(n - pog)$	1.32	1.4	1.46	1.4	1.41	1.3	1.32	1.5	1.34	1.4	1.34	0.01	0.06	3.96
$(t_m - g_{om})/(sn - pog)$	1.29	0.14	0.26	0.19	0.22	0.16	0.03	0.23	0.21	0.25	0.14	0.02	0.06	2.52

With the results of this method it's also possible to see an increasing of the nose width, of the posterior facial height and of the anterior facial height, as confirmed in the CCA approach. Another proof of the asymmetry found by this method is given by the goniac angles, wich increase from the pre surgery to the post surgery condition and presents a bigger value on the left side than the one in the right side. The angle $sls - \widehat{n} - sn$ shows an increased value between the pre and post surgery which means that the mandibular region has been moved ahead.

This three-dimensional approach has been able to give a global morphological shift evaluation of the soft-tissues without employing invasive procedures. Considering the necessity to give to the physician simple and direct informa-

290 tion, it seems the most efficient solution.

291 4.4 Clearance Vector Mapping

292 The CVM method has been applied aligning the point clouds with the three
293 invariant points of the Frankfort plane, then the distances have been calculated
294 with the most frequently used algorithm: the radial method. The distances are
295 shown by the colour maps in figure 11.

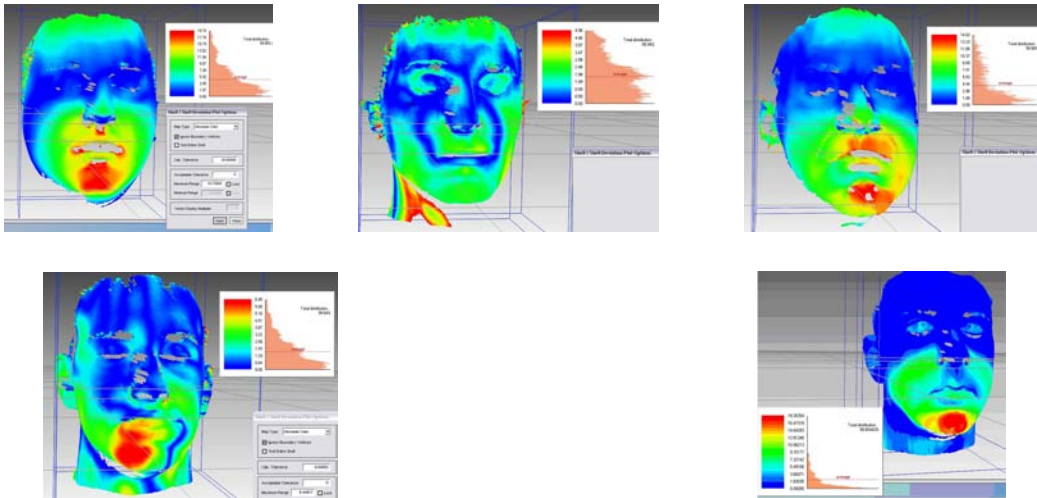


Figure 11. Clearance Vector Mapping graphical outputs.

296 This method can't manage the landmark measures, because it considers glob-
297 ally the displacement of the entire point cloud, but it is possible to validate
298 its results verifying if the colour map of the nose shows a clear indication of
299 the shape modification that has been found by the physician with the tradi-
300 tional method. Looking at the results (fig. 11) obtained with the five patients
301 analyzed, it is possible to understand that the method is not stable. It in fact
302 it shows for three case studies a significant modification of the mandibular
303 region, while for the other two, it presents other soft-tissue shifts or no move-
304 ments. This is probably due to the blindness of the method that compares

305 non homologous points between the two point clouds.

306 Also working with the normal or the closest methods it always associates a
307 point of the first point cloud with another on the second, that can be uncorre-
308 lated because of a definite shape change. Unfortunately the surgery causes a
309 complex modification of the face shape that often displaces the location from
310 the original location.

311 This method seems to be not useful for diagnostic purpose.

312 *4.5 Results comparison*

313 The most important considerations are summarized in table 6. CCA has been
314 left out because it is the well-known traditional method.

315 **5 Conclusions**

316 The analysis developed on the methods proposed in the technical literature
317 has evidenced the Multisectional Splines as the most reliable and most in-
318 formative about tissues shifts, because it is able to give reliable information
319 about the tissues shifts, as the CCA approach, but more than CCA is able
320 to give additional global information, as for instance the lateral asymmetry
321 verified in this paper employing the 3D point clouds.

322 But there are some significant points on which it is necessary to work to
323 develop a diagnostic procedure that could be accepted by the entire medical
324 context. It is necessary to define a method that extracts shape morphology
325 measures starting from the landmarks as reference points, so to guarantee

326 consistent morphological comparison, but also considering the entire facial
 327 shape (point cloud) so to consider each useful information. The morphological
 328 shape analysis tool must also provide reliable information and clear and simple
 329 outputs also for big dimensions samples.

330 6 Acknowledgements

331 The authors want to thank Prof. G. Ramieri and Prof. L. Verzè of the “Univer-
 332 sità di Torino” that collaborating with the authors in the LAFAV laboratory,
 333 financed by Compagnia di San Paolo, have provided precious suggestions and
 334 data for this study.

Table 6

Global comparison between the facial morphological analysis methods .

Method	Disadvantages	Advantages	Support
GPA	Not simple output Not reliable information Not global morphological analysis	Average facial shape evaluation	Point cloud
TPS	Very complex output Not global morphological analysis	Reliable information	Radiography
MS		Reliable Data Global morphological analysis Simple output	Point cloud
CVM	Not reliable data Not flexible method		Point cloud

335 **References**

- 336 [1] Ferrario V. F., Sforza C., Schmitz J. H., et al., Three-dimensional facial
337 morphometric assessment of soft-tissue changes after orthognathic surgery, *Oral*
338 *Surg Oral Med Oral Pathol Oral Radiol Endod*, 1999; **88**(5):549-556.
- 339 [2] Sforza C., Dellavia C., Tartaglia G. M., Ferrario V. F., Morphometry of the ear
340 in Down's syndrome subjects. A three-dimensional computerized assessment,
341 *Int J Oral Maxillofac Surg*, 2005; **34**:480-6.
- 342 [3] Chew M. T., Soft and hard tissue changes after bimaxillary surgery in Chinese
343 class III patients, *Angle Orthod*, 2005; **75**:959-63.
- 344 [4] Koh C. H., Chew M. T., Predictability of soft tissue profile changes following
345 bimaxillary surgery in skeletal class III Chinese patients, *J Oral Maxillofac*
346 *Surg*, 2004; **62**:1505-1509.
- 347 [5] Hoffmann J., Westendorff C., Leitner C., et al., Validation of 3D-laser surface
348 registration for image-guided cranio-maxillofacial surgery, *J Craniomaxillofac*
349 *Surg*, 2005; **33**(1):13-18.
- 350 [6] Katsumata A., Fujishita M., Maeda M., et al., 3D-CT evaluation of facial
351 asymmetry, *Oral Surg Oral Med Oral Pathol Oral Radiol Endod*, 2005;
352 **99**(2):212-20.
- 353 [7] Mori A., Nakajima T., Kaneko T., et al., Analysis of 109 Japanese children's lip
354 and nose shapes using 3-dimensional digitizer, *Br J Plast Surg*, 2005; **58**(3):318-
355 329.
- 356 [8] Sforza C., Dellavia C., Colombo A., et al., Nasal dimensions in normal subjects.
357 Conventional anthropometry versus computerized anthropometry, *Am J Med*
358 *Genet*, 2004; **130A**:228-233.

- 359 [9] Hajeer M. Y., Ayoub A. F., Millett D. T., Three-dimensional assessment of
360 facial soft-tissue asymmetry before and after orthognathic surgery, *Br J Oral*
361 *Maxillofac Surg*, 2004; **42**:396-404.
- 362 [10] Soncul M., Bamber M. A. Evaluation of facial soft tissue changes with optical
363 surface scan after surgical correction of Class III deformities, *J Oral Maxillofac*
364 *Surg*, 2004; **62**(11):1331-1340.
- 365 [11] McIntyre G. T., Mossey P. A., Size and shape measurement in contemporary
366 cephalometrics, *European Journal of Orthodontics* 2003; **25**:231-242.
- 367 [12] Harmon L. D., Khan M. K., Lashc R., Ramig P. F., Machine identification of
368 human faces, *Pattern Recognition* 1981; **13**(2):97-110.
- 369 [13] Tsang K. H. S., Cooke M. S., Comparison of cephalometric analysis using a non-
370 radiographic sonic digitizer (DigiGraph™ Workstation) with conventional
371 radiography, *European Journal of Orthodontics* 1999; **21**:1-13.
- 372 [14] Manual XLSTAT. <http://www.xlstat.com/en/support/tutorials/gpa.htm>
373 [Accessibility verified April 21, 2008]
- 374 [15] Swiderski D. L., Morphological evolution of the scapula in three squirrels,
375 chipmunks, and ground squirrels (Sciuridae): an analysis using thin-plate
376 splines, *Evolution* 1993; **47**:1854-1873.
- 377 [16] Richtsmeier J. T., Cheverud J.M., Lele S., Advances in anthropological
378 morphometrics, *Ann Rev Anthropol*, 1992; **21**:283-305.
- 379 [17] Bookstein F. L., Morphometrics tools for landmark data, Cambridge:
380 Cambridge University Press, 1991.
- 381 [18] Coombes A. M., Moss J. P., Linney A. D., Richards R, James DR. A
382 mathematical method for comparison of three dimensional changes in the facial
383 surface, *Eur J Orthod* 1991; **13**:95-110.

- 384 [19] Raby G. P., Current principles of morphoanalysis and their implementations in
385 oral surgical practice, *Br J Oral Surg*, 1977; **15**:97-109.
- 386 [20] Bush K., Antonyshyn O., Three-dimensional facial anthropometry using a
387 laser surface scanner: validation of the technique, *Plast Reconstr Surg* 1996;
388 **98**(2):226-235.
- 389 [21] Hyun C. D., Dong Y. I., Uk L. S., Registration of multiple-range views using
390 the reverse-calibration technique, *Pattern Recognition* 1998; **31**(4):457-464.
- 391 [22] Aung S. C., Ngim R. C., Lee S. T., Evaluation of the laser scanner as a surface
392 measuring tool and its accuracy compared with direct facial anthropometric
393 measurements, *Br J Plast Surg*. 1995; **48**:551-558.
- 394 [23] Ferrario V. F., Sforza C., Serrao G., Ciusa V., Dellavia C., Growth and aging
395 of facial soft-tissue: a computerised three-dimensional mesh diagram analysis,
396 *Clin Anat* 2003; **16**:420-33.
- 397 [24] Ferrario V. F., Sforza C., Ciusa V., Dellavia C., Tartaglia G. M., The effect
398 of sex and age on facial asymmetry in healthy subjects: a cross-sectional study
399 from adolescence to mid-adulthood, *J. Oral Maxillofac surg* 2001; **59**:382-388.
- 400 [25] Baumrind S., Frantz R. C., The reliability of head film measurements.
401 Landmark identification, *Am J Orthod* 1971; **60**:111-27.
- 402 [26] Houston W. J. B., Maher R. E., McElroy D., Sherriff M., Sources of error in
403 measurements from cephalometric radiographs, *Eur J Orthod* 1986; **8**:149-51.
- 404 [27] Baumrind S., Miller D. M., Molthen R., The reliability of head film
405 measurements. 3. Tracing superimpositions, *Am J Orthod* 1976; **70**:617-44.
- 406 [28] Dryden I. L., Mardia K. V., Statistical shape analysis. Chichester: J. Wiley,
407 1998

- 408 [29] Rohlf F. J., Slice D. E. Extensions of the Procrustes method for the optimal
409 superimposition of landmarks, *Systematic Zoology* 1990; **39**:40-59.
- 410 [30] Hajeer M. Y., Ayoub A. F., Millett D. T., Three-dimensional assessment of
411 facial soft-tissue asymmetry before and after orthognathic surgery, *Br J Oral*
412 *Maxillofac Surg* 2004; **42**:396-404.